EXPERIMENTAL AND MATHEMATICAL STUDY OF A HYDROGEN-OXYGEN FLAME

K. H. EBERIUS, K. HOYERMANN, AND H. GG. WAGNER

Institut für Physikalische Chemie der Universität Bochum und Göttingen, Göttingen, Germany

Fuel-rich premixed hydrogen–oxygen flames were stabilized on cooled porous plate burners at pressures around 10 mm Hg. The concentrations of H_2, O_2, H_2O, H, and OH were measured by means of mass spectroscopy, gas chromatography, uv-absorption spectroscopy, and ESR spectroscopy.

For one flame, the system of equations describing the propagation of the flame was solved numerically with respect to the interactions between the flame and the flameholder. These profiles, which were computed according to the boundary conditions and the kinetic data, are in agreement with the measured profiles.

A discussion on the accuracy of concentration and temperature measurements is given, taking into account diffusion, thermal diffusion, heat transfer, and "two-body collision" equilibrium.

From the experimental and mathematical work, it was found that, in these fuel-rich hydrogen–oxygen flames, water is produced at low temperatures by the chain mechanism

$$\begin{aligned} H + O_2 + M &\rightarrow HO_2 + M \\ H + HO_2 &\rightarrow OH + OH \\ OH + H_2 &\rightarrow H_2O + H, \end{aligned}$$

with the chain length of the order of 10. At high temperatures, water is produced by the branching mechanism

$$\begin{aligned} H + O_2 &\rightarrow OH + O \qquad (2) \\ O + H_2 &\rightarrow OH + H \\ OH + H_2 &\rightarrow H_2O + H. \qquad (1) \end{aligned}$$

The derived rate coefficients

$$k_1 = 1 \times 10^{13} \exp(-4800/RT); \quad 500°K < T < 1500°K$$

$$k_2 = 2.3 \times 10^{14} \exp(-16800/RT); \quad 650°K < T < 1000°K$$

(units in cal, mole/cm^3, °K) are in good agreement with rate constants reported in the literature.

Introduction

Flames are complex systems in which reactions, heat conduction, ordinary diffusion, thermal diffusion, flow, and heat transfer interact. They are understood in principle, but their quantitative description raises two difficulties. First "*ab initio*" calculations of burning velocities and concentration profiles are complicated; in addition, the reactions which occur, as well as the transport properties and their temperature dependence, must be completely known. Second, the proof of the analysis can only be given by exact measurement of the temperature, the concentrations, and the concentration gradients of all species that play an important role in the system.

The purpose of this paper is to give a survey of mathematical and experimental flame studies, based on a few examples of investigations of

simple H_2–O_2 low-pressure flames carried out in this laboratory over many years. In order to keep the paper short, only those details and results are included which are important for the discussion.

Direct measurements of concentrations in the flame zone, which do not disturb the flame, are scarcely feasible. Optical devices can be used to determine OH concentrations—and thereby the rotational temperature—whereas other species are determined by collecting samples from the flame for analysis: H and O atoms by ESR, the stable species O_2, H_2, and H_2O by mass spectroscopy and GC. The question of how well these samples represent the composition at a given reaction time can only be answered indirectly by several cross checks, such as a detailed mass balance for each atom species, energy balance, "two-body collision" equilibrium, etc. This is possible in some special cases. For example, when O and H atoms in the H_2–O_2 system are measured by ESR, the OH radical in the sampling system will remove O atoms via $O + OH \rightarrow O_2 + H$, leading to erroneous concentration of O and H atoms. When the OH concentration is measured independently by uv spectroscopy, and if it is small as compared with the O or H atoms, small corrections in the ESR measurements of the odd-electron species are possible.

The difficulties associated with the quantitative description of even a simple flame may be illustrated by a brief discussion of the differential equation and the boundary conditions. For a one-dimensional stationary flame, $(dn_i/dt)_r = dG_i/dz$ is the change of the concentration of a species i due to chemical reaction $G_i = n_i v - D_i\, dn_i/dz$, the mole flux of the species i, where Fick's law with the constant D_i is used and z, the coordinate of the flow, is positive in the direction of flow. These coupled differential equations are very sensitive to small round-off errors, if the direction of the integration is from the cold end of the flame to the hot end ($dz > 0$). For simplicity, the rate of reaction may be expressed as $(dn_i/dt)_r = k \cdot n_i$. Then, the two differential equations for the mole flux and the concentration of the species i are

$$dG_i/dz = -kn_i$$

$$dn_i/dz = (n_i v - G_i)/D_i.$$

Suppose the calculated value of n_i to be somewhat high. The first equation then gives a value for G_i which is somewhat less than the correct value. From the second equation, it follows that n_i increases again, especially as $n_i v$ is of the order of G_i. The small error increases exponentially. If n_i is calculated somewhat too low, the error increases again exponentially.

Integration from the hot end of the flame to the cold end is accompanied by other kinds of difficulties. For $z \rightarrow \infty$, all gradients are zero and the differential equations have a singularity there. If the boundary conditions are given for a certain z, they must be given with a very high accuracy in order to permit integration through the flame to the cold end. For example, let n_i be the small concentration of a radical at the boundary, r_+ the rate at which n_i forms, r_- the rate at which it disappears. Then for $r_+ \approx r_-$, $r \gg |r_+ - r_-|$, $dn_i/dt = dn_i/dz\, v = r_+ - r_- \approx 0$. Now, the error Δr in r must be smaller than $n_i/\Delta z\, v$, if it is not to lead to arbitrary values at the cold boundary (Δz is the path of integration), or

$$\Delta r/r \approx n_i/\Delta z \cdot v \cdot r.$$

Typical values are $v = 200$ cm/sec, $\Delta z = 5$ cm, $r = k\, n_i \cdot n_j$, with $k = 10^{13}$ cm^3/mole sec, $n_j = 10^{-7}$ mole/cm^3, which gives $\Delta r/r \approx 10^{-9}$. Because r is proportional to k, r_i, and r_j, both the rate constant and the concentrations at the hot end of the flame should have this accuracy.

These difficulties are overcome by treating the partial differential equations which describe the time-dependent propagation of a flame. As the structure of a flame depends upon the properties of the flameholder, the interactions between the flame and the flameholder have to be specified. The interactions are diffusion of heat, recombination of radicals, etc. Finally, one obtains the stationary solution of the flame for time going to infinity.

Guided by these considerations, the experimental setup was designed. By careful selection of the initial conditions, concentration and temperature data were obtained which can be related to profiles calculated by theories of flame propagation.

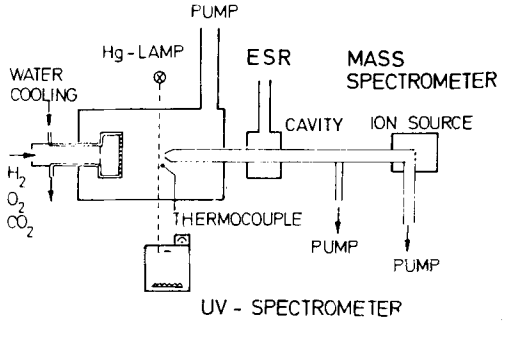

FIG. 1. Experimental setup for measuring concentrations of stable and unstable species in flames.

Experimental Setup and Measurements

Figure 1 is a diagram of the experimental setup. The burner housing was made from aluminum with a movable flameholder that penetrated from the front horizontally into the housing. (Aluminum, as a nonmagnetic material, was necessary in order to bring the burner as near as possible to the cavity and the ESR magnet.)

The flame was stabilized on a cooled porous bronze plate. The side walls of the housing were equipped with windows of quartz to permit

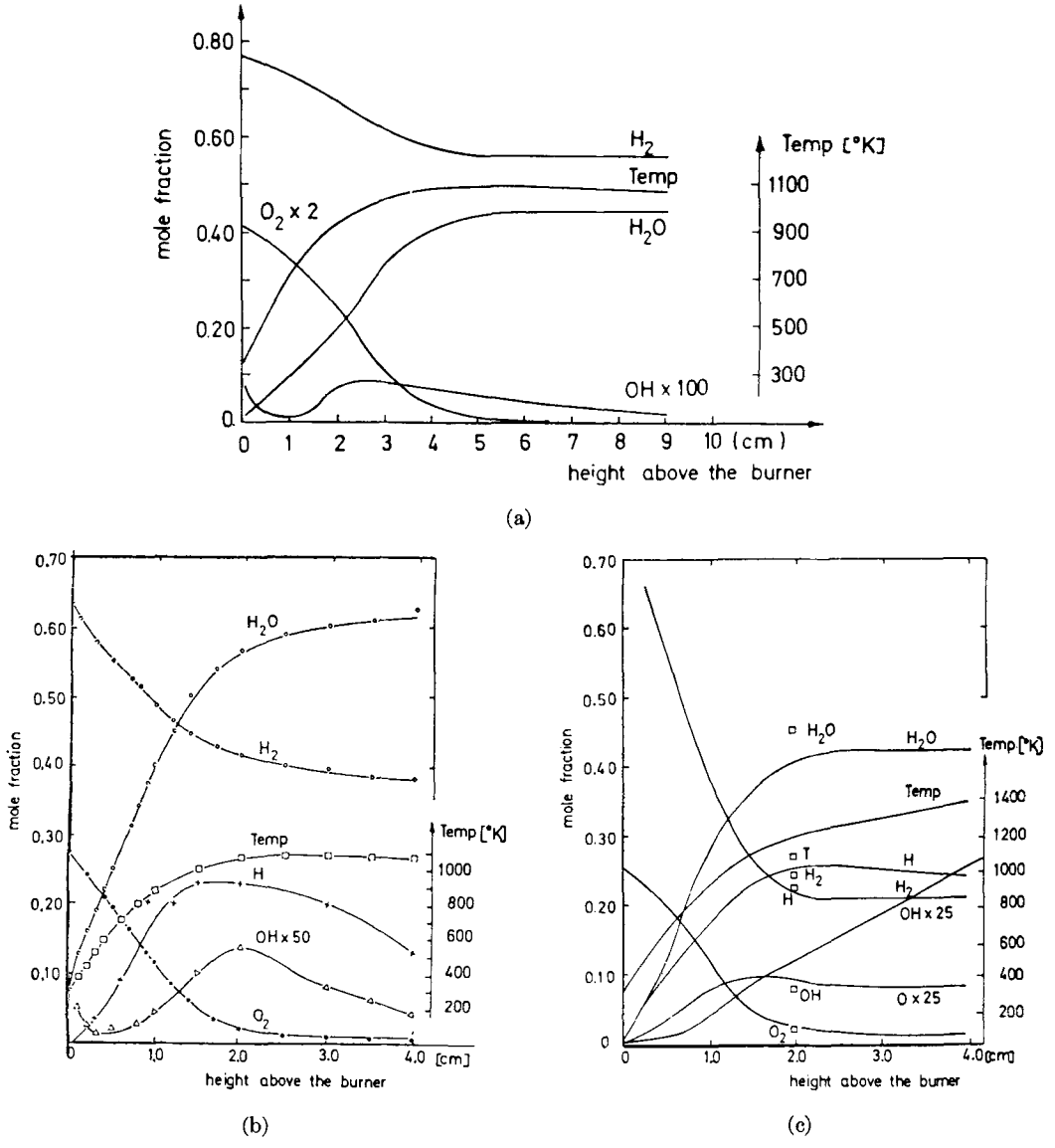

FIG. 2. Temperature and concentration profiles of H_2–O_2 flames. (No corrections have been made for recombination reactions in the sampling system.)

(a) Measured:
81 mole % H_2/19 mole % O_2; v_0 = 156 cm/sec, p = 7.7 mm Hg; burner diameter, 19 cm.

(b) Measured:
75 mole % H_2/25 mole % O_2; v_0 = 178 cm/sec, p = 10.6 mm Hg; burner diameter, 7.5 cm.

(c) Calculated:
75 mole %$_0$$H_2$/25 mole % O_2; v_0 = 178 cm/sec, p = 10.6 mm Hg; burner diameter, 7.5 cm.

□ indicates measured values [Fig. 2(b)].

optical measurements, especially measurement of the rotational temperature and the concentration of OH. The optical arrangement was such that the concentration gradients in the flame did not influence the intensity of the light transmitted to the spectrometer. A thermocouple (covered with quartz, 0.3 mm diam) was introduced from above. The losses of radiation could be compensated by electrical heating. A quartz probe, introduced from the side facing the flameholder, was used to transfer gas samples from the flame to the cavity of an ESR spectrometer by the method of Westenberg and Fristrom,[1] and to a mass spectrometer with a continuous intake. The inner diameter of the probe was 1 cm, and the distance from the tip to the cavity was at least 15 cm. The cavity and the magnet of the ESR could be moved along the sampling tube (40 cm), thus making it possible to determine H- and O-atom concentrations at the probe tip by extrapolation of the measured values.

Temperature and concentration profiles were obtained by moving the flameholder by means of a spindle. Gases were metered by capillary flowmeters.

In a second device,[2] which was not designed for ESR measurements, a cooled porous plate of sintered bronze served as a 19-cm-diam flameholder. A 3-mm-diam quartz probe was introduced laterally into the flame at an angle of about 45°. The gas samples withdrawn from this burner were analyzed for H_2, O_2, H_2O, N_2, CO, and CO_2 by gas chromatography.

The experimental conditions were selected to provide

a large zone of reaction,
a low final temperature,
strong stabilization of the flame,
simplicity of the reaction mechanism,
a small number of reactants,
knowledge of reactions in the probe, and an OH concentration $\approx 10^{-3}$ mole fraction.

As a compromise, a fuel-rich hydrogen–oxygen flame was chosen with the following values for the composition and the velocity of the unburned gas and for the pressure: 19-cm burner (81% H_2/19% O_2, 156 cm/sec, 7.7 mm Hg), 7.5-cm burner (75% H_2/25% O_2, 178 cm/sec, 10.6 mm Hg). The stabilization of the flame—that is, the adjustment of the velocity of the unburned gas—was chosen so that the inflection point of the temperature profile coincided with the surface of the burner.

Figures 2(a) and 2(b) show various profiles obtained with these arrangements. In these figures, the profiles of H_2, O_2, and H_2O are not corrected for recombination of radicals in the probe.

The OH concentration was measured by absorption spectroscopy.[2] The H-atom concentration was measured by ESR spectroscopy.[3]

The O-atom concentration could not be obtained with reasonable accuracy, due to rapid reaction in the probe. (The measured concentration was less than 0.05 mole %.)

Computation of a Flame Stabilized on a Flameholder

The given treatment always considers a one-dimensional premixed flame. The flame was computed by the method proposed by Spalding,[4] and applied by Adams and Cook[5] to the model of a hydrazine flame, and by Dixon-Lewis[6] to a hydrogen–oxygen flame. This method uses the equations which describe the propagation of a flame into quiescent unburned gas. The temperature and the concentrations are functions of space and time. The desired solution of the stationary flame then becomes the state seen by an observer moving with the flame when time is going to infinity. This method has the advantage that these equations, which are partial differential equations, are not so sensitive to round-off errors as the ordinary differential equations which describe the stationary flame. For the equations of stationary flames and solution of singularities, the reader is referred to Hirschfelder, Curtiss, and Bird.[7] The present calculations follow the work of Dixon-Lewis,[6] and the equations describing the propagation of the flame are not repeated here.

The boundary conditions for the nonstationary case must be specified in such a way that they are equivalent to the boundary conditions for a stationary flame stabilized on a flameholder. In the stationary case, the unburned premixed gas flows with a given velocity v_h through the flameholder, which is at rest. This changes to a flame-

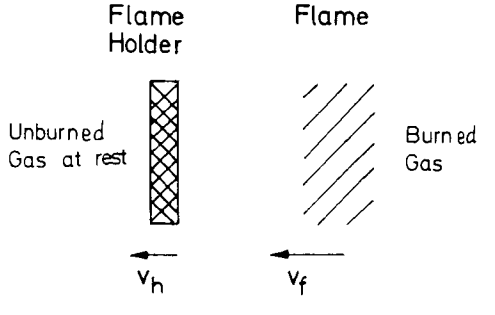

FIG. 3. Model for the propagation of a flame stabilized on a flameholder. v_h = flameholder velocity, v_f = flame velocity.

holder moving with the velocity v_h through the unburned gas (Fig. 3). The flameholder is permeable only to the unburned gas. If the flame is ignited anywhere downstream of the flameholder, it propagates initially with the free-flow velocity v behind the flameholder ($v > v_h$). However, the flame cannot outrun the flameholder, which in the stationary case would be a flashback of the flame. The flameholder prevents diffusion of heat and active particles into the unburned gas. The burner withdraws heat and active particles from the flame, reducing its speed until it has the same velocity as the flameholder ($v = v_h$). The flame is then stationary with respect to the flameholder. As the flameholder is impermeable to diffusing particles, these diffusion fluxes must be added to the unburned gas. Recombination of radicals at the surface of the flameholder must be taken into account. The boundary conditions at the hot end ($z \rightarrow \infty$) of the flame are automatically the thermodynamic equilibrium of the reactants, otherwise there are no special requirements as, for example, a "double-collision equilibrium." The velocity of the burned gas for reactions, without change in the number of particles, is $v_\infty = v_h(T_\infty - T_0)/T_0$, where T_∞ = temperature of the burned gas, T_0 = temperature of the unburned gas.

As an example, a hydrogen–oxygen flame was computed that corresponds to one of the flames analyzed experimentally. The composition of the unburned gas was 75% H_2/25% O_2, its velocity was $v = 178$ cm/sec, and its pressure was $p = 10.6$ mm Hg. The reaction scheme was:

$$OH + H_2 \rightarrow H_2O + H \quad (1)$$

$$H + O_2 \rightarrow OH + O \quad (2)$$

$$O + H_2 \rightarrow OH + H \quad (3)$$

$$OH + OH \rightarrow H_2O + O \quad (4)$$

$$O + O + M \rightarrow O_2 + M \quad (5)$$

$$H + H + M \rightarrow H_2 + M \quad (6)$$

$$OH + H + M \rightarrow H_2O + M \quad (7)$$

$$H + O_2 + M \rightarrow HO_2 + M \quad (8)$$

$$H + HO_2 \rightarrow OH + OH. \quad (9)$$

The appropriate rate constants were taken from the literature (compilation by Schofield[8]). Third-collision partners were specified. The simplifications made are the same as those introduced by Dixon-Lewis, that is, the diffusion was treated as binary, neglecting thermal diffusion, and the coefficient of heat conduction was set proportional to the temperature. Figure 2(c) shows the profiles computed in this way.

Discussion

There is no experimental condition which is ideal in every respect. A large zone of reaction implies departures from the one-dimensional concept, a high temperature is coupled with large gradients, etc. The following considerations are not a discussion of errors, from which the accuracy of the rate constants could be derived *a priori*. On the contrary, the accuracy of the results could be used to discuss the accuracy of the experiments and of the assumptions made when evaluating the data. Error estimations made *a priori* are, in most cases, so rough that their limits exceeds the value of the results. The accuracy of the various parameters varies from point to point in the flame. For detailed discussions of the parameters of flame experiments one should refer to Fristrom and Westenberg,[9] who also give further references.

The OH concentration was measured optically, the absorption recorded is an average along the path of the light, and the accuracy of converting the absorption into concentration depends on the structure of the flame. The flame was assumed to be one-dimensional, which holds near the flameholder. Especially for this reason, a strong stabilization of the flame is important. Departures from the equilibrium distribution of the OH rotational levels may be an indication that the light samples OH molecules at different temperatures. An error in the OH concentration causes the same error in the corresponding rate constants (20%).

For the present experiments, it was satisfactory to sample H atoms with a quartz probe, and to analyze them by ESR spectroscopy. The H-atom concentration of this flame exceeds the concentration of the other radicals, so that reactions of O and OH with H in the probe cannot change the H concentration drastically (1% deviation at $z = 20$ mm, 0.01% at $z = 5$ mm). The measured H-atom profile is in good agreement with the computed profile.

Another possible check for consistency is the equilibrium established between binary collision reactions in the later parts of a flame,

$$k_+[OH][H_2] \approx k_-[H_2O][H]$$

or

$$K(T)[OH][H_2]/[H][H_2O] \approx 1,$$

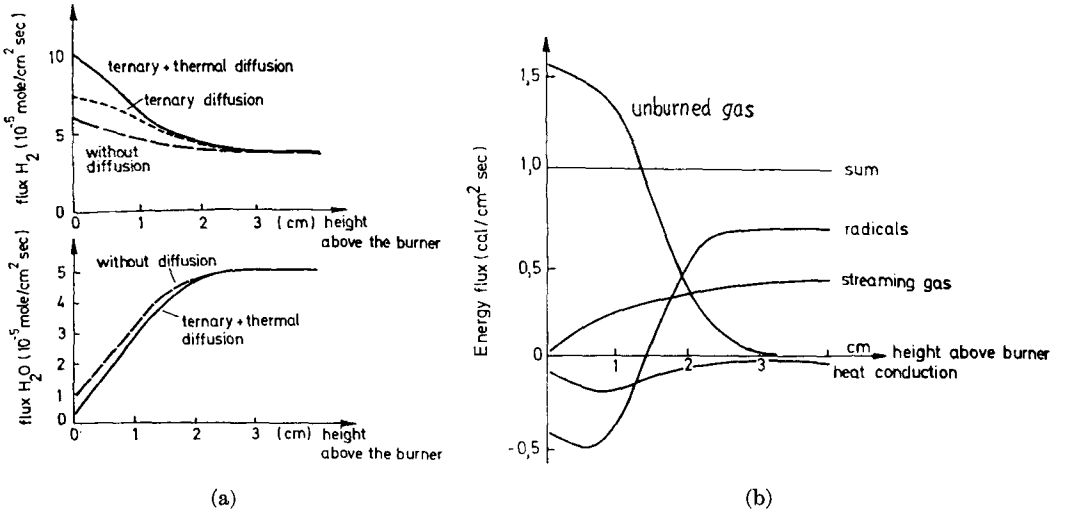

FIG. 4. Mass and energy balances.

(a) Mole fluxes of H_2 and H_2O of H_2/O_2 flame [Fig. 2(b)].
——, neglecting diffusion;
– – –, ternary diffusion included;
——, ternary and thermal diffusion included.

(b) Energy fluxes in H_2/O_2 flame [Fig. 2(c)]. Reaction enthalpies for H_2 and H_2O were taken to be zero and 115 kcal/mole for O_2.

where the equilibrium constant $K(T) = k_+/k_-$ changes by 10% if the temperature changes 10°K at 1000°K. The ratio gives a correlation between the H concentration, the OH concentration, and the temperature, which were measured independently, and gave the ratio of 1 within 30%.

H atoms recombined on their way to the mass spectrometer. This reduced the number of particles of the sample and increased the concentration of all other stable species. In subsequent calculations, the measured concentrations were recalculated, assuming that the H atoms recombine to H_2.

O-atom profiles could not be measured with the ESR, because they react to give other products, presumably H_2O, before they reach the ESR cavity. This may cause an error in the H-atom concentration of 20% if the O atoms react only with H atoms.

The concentration of the gas samples was measured very accurately by the mass spectrometer with a continuous intake. The spectrometer readings were converted separately to concentrations. The difference of the sum of all mole fractions from 1 was always within 0.02.

The great influence of diffusion, especially in the prereaction zone, was demonstrated by adding 1% He and 1% Ar, which do not take part in the reaction. Whereas the mass balance of Ar (as a tracer for heavy molecules) was measured correctly, the profile of He (as a tracer for light molecules) showed strong deviation due to diffusion in the direction of the burner. Quantitative calculations, taking into account diffusion terms, are shown for the fluxes of H_2 and H_2O (flame: 75% H_2/25% O_2) in Fig. 4(a). Ternary diffusion was assumed for a mixture of H_2–O_2–H_2O, where the H atoms were regarded as a part of H_2. As can be seen, thermal diffusion of H_2 predominates in the diffusion-governed pre-reaction zone. When these results are compared to the measured concentrations [Fig. 2(b)], a discrepancy of a few percent is observed. This is explained by the fact that, at low temperatures (i.e., small diffusion coefficients), the concentrations measured by sampling are better represented by mole fraction than by mole flux.

The H_2O profile [Fig. 2(b)] at $z = 0$ is reduced to one-third when diffusion is taken into account.

Regarding diffusion explicitly, it is understood that the measured H_2 concentration of Fig. 2(b) at $z = 0$ (63%) corresponds quantitatively to the initial concentration of 75 mole % H_2.

Probe sampling is a serious problem. The measurements in the 7.5-cm flame were made with the 1-cm-diam quartz probe introduced from the hot end of the flame, and the gas was removed at approximately the flux of gas through the cross section of the probe in the free stream. In the hot parts of the flame, the probe sampled less

gas because the gas was more viscous. Comparison of the resulting profiles with the computed profiles suggests that the samples extracted by the probe may be largely representative of the concentrations of the components in the flame. The distortions caused by the 1-cm probe in the diffusion-controlled regime of the flame, with large temperature gradients and little chemical reaction, were so large that the temperature profiles could not be matched with the concentration profiles of the various components accurately enough to evaluate rate constants. The conditions for obtaining rate constants are much better in the hot part of the flame, where the temperature gradient is smaller and chemical reaction predominates over diffusion. Better accuracy was achieved in the diffusion regime with the smaller probe in the 19-cm flame.

The temperature measured by the thermocouple was in agreement with the rotational temperature of OH when measured either at the cold end or the hot end of the flame. In the main reaction zone, the rotational temperature gave values up to 30°K higher, accompanied by a nonequilibrium distribution of the rotational levels. This could be due to an effect from the outer parts of the flame.

Another possibility for checking the accuracy of the measurements (concentration, temperature) is to evaluate the rate constants from the measured flames. Here, concentrations of radicals and stable products and temperatures contribute significantly to the results. If the rate expressions derived from the measured profiles (Fig. 2) agree with the rates found by other methods, this can be regarded as a criterion for the consistency of the concentration and temperature data.

Reaction (1) was followed by evaluating the H_2O profile. Estimates show that other reactions, such as

$$OH + OH \rightarrow H_2O + O,$$

$$OH + HO_2 \rightarrow H_2O + O_2,$$

$$OH + H + M \rightarrow H_2O + M,$$

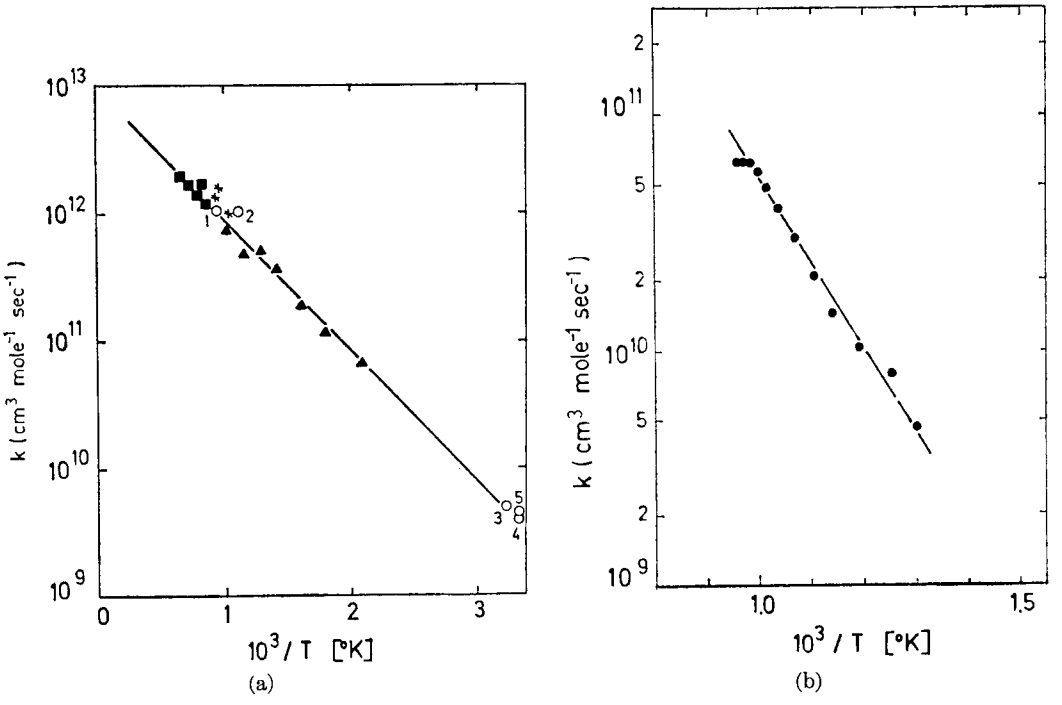

FIG. 5. Arrhenius plot for reaction rates as evaluated from H_2/O_2 flames.

(a) $OH + H_2 \rightarrow H_2O + H$,

$k_1 = 1 \times 10^{13} \exp(-4800/RT)$ cm³/mole sec.

▲, evaluation from flame of Fig. 2(a).

■, evaluation from 0.48 H_2/0.52 O_2 flame; p = 7.24 mm Hg, v_0 = 223 cm/sec;

* evaluation from flame of Fig. 2(b).

○1 and ○2, Ref. 13; ○3, Ref. 12; ○4, Ref. 11; ○5, cited in Ref. 13.

(b) $H + O_2 \rightarrow OH + O$, evaluated from flame of Fig. 2(b). $k_2 = 2.5 \times 10^{14} \exp(-16800/RT)$ cm³/mole sec.

can be neglected above 500°K. With the reverse reaction, water is produced by

$$d[H_2O]/dt = k_+[OH][H_2] - k_-[H_2O][H].$$

The reverse reaction can be neglected in the first part of the flame. The rate of H_2O production was computed from the H_2O profile assuming that the water diffuses in a mixture of hydrogen and oxygen. This assumption holds in the region where diffusion is most important, and especially for the conditions of the 19-cm flame. The fluxes of diffusion, thermal diffusion included, were computed for the three-component mixture, according to Hirschfelder, Curtiss and Bird.[7] The H-atom concentration in the later part of the 19-cm flame was considered to be constant and was calculated from the equilibrium at the end of the flame. The equilibrium $K = k_+/k_-$ was computed from thermodynamic data (JANAF[10]).

Figure 5(a) shows the values of the rate constant calculated in this way, together with results for another flame (48% H_2/52% O_2). Taking the above results together with results at room temperature obtained by Dixon-Lewis, Wilson, and Westenberg,[11] Kaufmann and Del Greco,[12] and Wise (see Ref. 13), the temperature dependence of the rate constant is

$$k_{1+} = 1.0 \times 10^{13} \exp(-4800/RT) \text{ mole/cm}^3 \text{ sec}.$$

Two reactions are discussed which consume oxygen, Reactions (8) and (2). With a rate constant of 10^{17} cm^9/mole^2 sec for Reaction (8), and for the conditions of the 7.5-cm flame, the rates of both reactions are equal at 800°K. Figure 5(b) shows the evaluation of the rate constant for the second reaction, where diffusion was handled in the same manner as for H_2O. The result indicates no influence of the O-atom recombination in the probe on the O_2 profile. The rate constant of

$$k_2 = 2.3 \times 10^{14} \exp(-16{,}800/RT) \text{ cm}^3/\text{mole sec}$$

is in good agreement with the values reported so far in the literature.[9] For Reaction (8), a rate constant of $k = 3 \times 10^{16}$ cm^6/mole^2 sec at $T =$ 600°K was estimated from the decay of the O_2 profile. The third-collision partner was not specified.

The $O + H_2 \rightarrow OH + H$ reaction could not be calculated from the profiles, since the decay of H_2 is also due to the reaction with OH. In view of the sampling technique, the H_2 concentrations are not as accurate as the other concentrations. The H_2 concentration is greatly influenced by recombination of radicals in the probe, and is not accurate enough to allow a complete separation of both reactions.

The $CO_2 + H \rightarrow CO + OH$ reaction was studied in another fuel-rich hydrogen–oxygen flame, with 3% CO_2 added. The contributions of diffusion to the rate of reaction were negligible. These measurements lead to a value of $k_{10} = 1.3 \times 10^9$ cm^3/mole sec at $T = 1050$°K, which agrees well with the data calculated from the reverse reaction.[11,13,14]

From the remarks on sampling, diffusion terms, etc., it is obvious that no reliable data for the temperature dependence of elementary reaction near room temperature can be derived. However, a general picture can be deduced for this pre-reaction zone. For this region, Fenimore and Jones,[15] and Dixon-Lewis, Sutton, and Williams[16] postulate the Reaction (8) without specifying the further reaction mechanism. The existence of the HO_2 radical in fuel-rich H_2–O_2 flames was shown by mass-spectroscopic measurements of Homann and Wagner.[17]

Our measurements and calculations give the H-atom concentration, the water formation, and the influence of diffusion. Based on this, it appears that, in the low-temperature region, the course of the reaction is governed by the following chain reaction

$$H + O_2 \xrightarrow{M} HO_2 \qquad (8)$$

$$H + HO_2 \rightarrow 2\,OH \qquad (9)$$

$$OH + H_2 \rightarrow H_2O + H, \qquad (1)$$

giving a chain length of 10 in the case of the computed flame, and 20 when deduced from the measured (75% H_2/25% O_2) flame.

This result is in agreement with the observations mentioned above.[15,16]

A balance of the energy fluxes with reaction time [Fig. 4(b)] is given for the flame of Fig. 2(c), where the fluxes are specified for heat conduction, enthalpy of the flowing gas, enthalpy of reaction for the radicals and of the unburned gas. (For the reference point of energy, see the figure caption.) Since negative fluxes in this figure indicate energy transport in the direction of the flameholder, it can be seen that a lot of energy is transferred to the flameholder at an early stage of the reactions.

This is in good agreement with the mechanism in the preheating zone as discussed above.

Acknowledgments

The continuing interest of Prof. W. Jost, and financial support by the Stiftung Volkswagenwerk

and the Deutsche Forschungsgemeinschaft are gratefully acknowledged.

REFERENCES

1. WESTENBERG, A. A. AND FRISTROM, R. M.: *Tenth Symposium (International) on Combustion*, p. 473, The Combustion Institute, 1965.
2. BONNE, U., GREWER, TH., AND WAGNER, H. GG.: Z. phys. Chem. N.F. *26*, 93 (1960).
3. HOYERMANN, K. H., WAGNER, H. GG., AND WOLFRUM, J.: Ber. Bunsenges. Physik. Chem. *71*, 599 (1967).
4. SPALDING, D. B.: Phil. Trans. *A249*, 1 (1956).
5. ADAMS, G. K., AND COOK, G. B.: Combust. Flame *4*, 9 (1960).
6. DIXON-LEWIS, G.: Proc. Roy. Soc. (London) *A298*, 495 (1967).
7. HIRSCHFELDER, J. O., CURTISS, C. F., AND BIRD, R.: Molecular Theory of Gases and Liquids, Wiley, 1954.
8. SCHOFIELD, K.: Planetary Space Sci. *15*, 643 (1967).
9. FRISTROM, R. M. AND WESTENBERG, A. A.: Flame Structure, McGraw-Hill, 1965.
10. JANAF Thermochemical Tables, Dow Chemical Co., Midland, Michigan, 1965.
11. DIXON-LEWIS, G., WILSON, W. E., AND WESTENBERG, A. A.: J. Chem. Phys. *44*, 2877 (1966).
12. KAUFMANN, F. AND DEL GRECO, F. P.: *Ninth Symposium (International) on Combustion*, p. 659, Academic Press, 1963.
13. DIXON-LEWIS, G., SUTTON, M. M., AND WILLIAMS, A.: Trans. Faraday Soc. *61*, 255 (1965).
14. JOST, W., SCHECKER, H. G., AND WAGNER, H. GG.: Z. Physik. Chem. (Frankfurt) *45*, 47 (1965).
15. FENIMORE, C. P. AND JONES, G. W.: *Tenth Symposium (International) on Combustion*, p. 489, The Combustion Institute, 1965.
16. DIXON-LEWIS, G., SUTTON, M. M., AND WILLIAMS, A.: *Tenth Symposium (International) on Combustion*, p. 495, The Combustion Institute, 1965.
17. HOMANN, K. H. AND WAGNER, H. GG.: DECHEMA Bericht, 1961.

COMMENTS

W. J. Miller, AeroChem Research Labs. The deviation of measured flame temperatures from the adiabatic values are apparently quite large. What are the adiabatic temperatures in your flames, and can the deviations be best accounted for in terms of heat losses to the burner and surroundings or are they due to the slowness of radical recombination reactions at these low pressures? If the latter is the case, can any limiting values of the three-body radical-recombination coefficients be inferred from the data?

Authors' Reply. Assuming thermodynamic equilibrium, the maximal flame temperatures of the hydrogen–oxygen flames considered here are about 2500°K. No rate data for recombination reactions were determined from these flames. (See, however, $H + H + H_2O \rightarrow H_2 + H_2O$.[1])

The energy production and the losses in the flame (Fig. 2b) were determined for the main reaction zone (0–20 mm height above the burner). The energy given to the burner (in cal/cm² sec) by heat conduction is 0.15, and by recombination reactions to the flameholder 0.44. To raise the temperature from 300°K to 1050°K, 0.63 cal/cm² sec, and for the production of radicals, 1.30 cal/cm² sec are required. The sum of 2.52 cal/cm² sec for the energy consumed corresponds within 8% to the energy production of −2.75 cal/cm² sec, calculated from the water production. As reported in the paper, an important part of the energy production in these flames proceeds via HO_2.

Reference

1. K. H. EBERIUS, K. HOYERMANN, AND H. GG. WAGNER: Ber. Bunsenges. Physik. Chemie *73*, 962 (1969).

L. F. Jesch, Sun Oil Co. In your experimental measurements, did you determine gas velocity in the reaction zone both radially and axially, in order to establish a time scale of events as the velocity changes with distance in the reaction zone, and did you find large gradients?

Authors' Reply. As shown for other flames, no large gradients are to be expected from the large ratio of main reaction length (20 mm height above the burner) to porous-burner diameter of 75 mm and 190 mm at low pressure.

When taking samples from the flame, from above and under different angles from the side, no differences in gas composition over nearly the entire flameholder were detected by mass spectrometry and gas chromatography. Besides this fact, an admixing of a few percent hydrocarbons (acetylene, ethylene) to the flame caused a flat and homogeneous luminous zone, indicating no large gradients.